Effect of X-rays on the Surface Chemical State of Al_2O_3, V_2O_5, and Aluminovanadate Oxide

S. P. Chenakin,[†,§] R. Prada Silvy,[‡] and N. Kruse*[,†]

Université Libre de Bruxelles (ULB), Chimie Physique des Matériaux, CP243, Campus Plaine, B-1050 Bruxelles, Belgium, and Université Catholique de Louvain, Croix du Sud 2, Boite 17, 1348 Louvain-la-Neuve, Belgium

Received: April 14, 2005; In Final Form: June 2, 2005

The surface composition of Al_2O_3, V_2O_5, and aluminovanadate oxide, "V−Al−O", was studied by X-ray photoelectron spectroscopy (XPS), using Mg K_α to reveal time-dependent irradiation damage of samples. Spectral parameters such as peak intensity and width and absolute and relative peak binding energies were evaluated along with the Auger parameter. Irradiation of Al_2O_3 was found to cause partial dehydration of the surface hydroxide film, while sputter-cleaned alumina turned out to be resistant to X-rays. In V_2O_5, a small fraction of V^{4+} species was seen to form during X-ray exposure. X-ray induced damage in Al_2O_3 and V_2O_5 was compared to that caused by bombardment with 500 eV argon ions. The V−Al−O material which is used as a precursor of oxynitride catalysts for ammoxidation turned out to be most susceptible and could be damaged by low X-ray doses. An appreciable reduction from the V^{5+} to the V^{4+} formal oxidation state (the latter increases from 20 to 45% after 150 min time of exposure to Mg K_α at 150 W) was found along with the decomposition of aluminum hydroxide which is believed to act as an amorphous support in this catalyst. Gas-phase analysis during X irradiation demonstrated desorption of oxygen and water molecules. X-ray induced damage is believed to be caused by electron−hole pair generation and Auger decay rather than by thermal effects since the sample surface temperature increased only slightly.

1. Introduction

X-ray photoelectron spectroscopy (XPS) is being successfully employed for the analysis of native oxides of metals and alloys, of binary and multicomponent bulk oxides, oxide glasses, or for the investigation of processes such as the oxidation of metallic materials and the growth and formation of thin-film oxides.[1] In particular, XPS may provide clues in the determination of the surface chemical composition, chemical state, and electronic structure of binary and mixed oxide catalysts.[2]

Way back in the 1970s, it was first reported[3] that the photoelectron spectra of molybdenum oxide, MoO_3, were affected by X irradiation. Accordingly, with time of exposure to X-rays, reduced intermediate structures, MoO_x ($2 < x < 3$), were observed to form at the surface of MoO_3. Only a few works have addressed radiation-induced damage ever since. A systematic study of the effect of Al K_α X irradiation on the surface composition was carried out by Paparazzo et al.[4,5] for CeO_2. The same authors found that increasing X-ray exposure caused partial chemical reduction of CeO_2 to a Ce_2O_3-like phase in a surface layer of 15−20 Å thickness. Having shown that some of the XPS features usually referred to as excited electronic states of ceria were, in fact, X-ray induced, they settled the controversy as to the true Ce3d spectrum. In a subsequent XPS study of sintered and nonsintered pellets of CeO_2 subjected to Al K_α X-rays, the irreversible radiation-induced reduction of ceria to Ce_2O_3 and possibly to other substoichiometric oxides was also observed.[6] The authors claimed that the reduction depended on the decomposition of hydroxyl species and that the thickness of the damaged layer extended beyond the depth probed by XPS. However, these statements were disputed.[7]

Vanadium pentoxide, widely used as a catalyst in industry for a variety of chemical reactions, has been extensively investigated by different ion and electron spectroscopic techniques. XPS analysis revealed that V_2O_5 is very sensitive to electron irradiation and can be reduced to lower oxidation states even by low-energy electron beams, so that electron spectroscopies should be used deliberately if accurate measurements are required.[8−10] However, it was observed that X-rays during XPS analysis could also modify the surface of V_2O_5.[10,11] Al K_α X irradiation of both single-crystal and polycrystalline V_2O_5 with a small amount of surface cadmium gave rise to the emergence of vanadium species in a lower oxidation state.[12]

For more complex systems such as multicomponent oxides, the effect of X irradiation becomes more sophisticated. Accordingly, a mixed oxide catalyst $V_2O_5-WO_3/TiO_2$ was more stable than V_2O_5/TiO_2 and no reduction of V^{5+} was detected under X irradiation, at least for two sequential XPS acquisition runs.[13] On the contrary, an enhanced reducibility of vanadia under XPS conditions was suggested[14] for ternary $V_2O_5-WO_3/TiO_2$ catalysts as compared with binary V_2O_5/TiO_2 catalysts. In the work of ref 15, a catalyst prepared by nitridation of aluminovanadate oxide precursor was studied by XPS, and the authors claimed that it remained stable both under Al K_α X irradiation and under 10 eV electron flood gun irradiation for up to 7 h. In an XPS study of aluminovanadate oxide precursors,[16] the high sensitivity of the catalyst to X irradiation was noted. In view of the extensive use of XPS for the identification of different oxidation states in bulk and supported oxide catalysts before and after catalytic reactions, following reduction in various environments, it is important to know the

* Author to whom correspondence should be addressed. Fax: +32-2-650 57 08; e-mail: nkruse@ulb.ac.be.
† Université Libre de Bruxelles.
‡ Université Catholique de Louvain.
§ Permanent address: Institute of Metal Physics, Nat. Acad. Sci., Vernadsky Blvd. 36, 03680 Kiev-142, Ukraine.

10.1021/jp051944j CCC: $30.25
Published on Web 07/13/2005

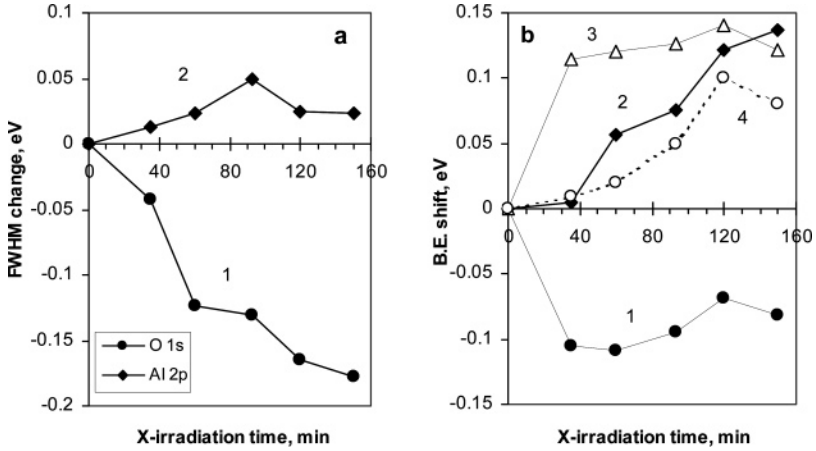

Figure 1. Change in fwhm (a) and binding energy shift (b) for the O 1s (1), Al 2p (2), and C 1s (3) peaks as a function of time of exposure of Al_2O_3 to X-rays with reference to a nonirradiated sample. The time-dependent shift of B.E. of the O1 peak (Figure 3) representing the Al−O−Al environment is also shown (4).

comparative stability of different oxide catalysts under X irradiation with respect to reduction. The aim of the present work is to investigate by XPS the modification of the surface state of aluminovanadate oxide, "V−Al−O", as a function of X-ray exposure and to compare the effect of X irradiation with reference oxides V_2O_5 and Al_2O_3.

2. Experimental Section

Aluminovanadate oxide was synthesized by coprecipitation from a solution of aluminum nitrate $Al(NO_3)_3 \cdot 9H_2O$ and ammonium metavanadate NH_4VO_3 with a ratio of V/Al = 0.25 (at. %) at pH = 7.5 adjusted by addition of a NH_4OH solution.[16] The precipitate was filtered, washed several times with hot water, and dried at 120 °C overnight, yielding finally a powder with an average size of the particles of about 230 μm. V−Al−O samples for XPS analysis were prepared either by sedimentation of the powder impregnated with pure 2-propanol on a stainless steel backing or by compacting the powder uniformly over an indium film on the sample holder to form a layer typically about 0.1-mm thick. No significant differences in the results were found for the samples prepared by either method. However, the latter was more convenient and reliable (because the high density of the compacted sample yielded higher intensities of measured signals and ensured more homogeneous surface charging) so that it was mainly employed. V_2O_5 powder (99.6%, Janssen Chimique) and sapphire wafer (α-Al_2O_3) were used as reference samples and studied for comparison.

Experiments were performed in a combined XPS-ToF-SIMS instrument at a base pressure of $1.2 \cdot 10^{-9}$ mbar. A non-monochromatic Mg K_α radiation was used at an operating power of 15 kV × 10 mA. Prior to analysis, the samples were outgassed for 160 h in a preparation chamber at a base pressure of $5 \cdot 10^{-10}$ mbar. The photon beam was incident at an angle of 19° to the sample surface normal thereby illuminating a sample area of about 0.4 cm^2. Photoelectron spectra were acquired with a hemispherical analyzer (at a takeoff angle of 50°) in the constant-pass-energy mode at Ep = 50 eV. The overall resolution of the spectrometer in this operating mode was 0.96 eV as measured by the fwhm of the $Ag3d_{5/2}$ line. The spectrometer was calibrated against $E_b(Au4f_{7/2}) = 84.0$ eV and $E_b(Cu2p_{3/2}) = 932.4$ eV. The Al *KLL* Auger spectra were recorded in the Bremsstrahlung radiation. If necessary, the binding energies of the oxides were corrected for surface charging by referencing to adventitious carbon C 1s at 285 eV. Measurements were carried out as a function of time of exposure to X-rays at room temperature for 3 h. Acquisition of core-level spectra was started immediately after the sample was moved under the running X-ray source, and the spectrum acquired first was defined as corresponding to a virgin surface and "zero-time" exposure. The temperature at the surface of the V−Al−O oxide sample was monitored with a Ni−NiCr thermocouple pressed into the powder layer. The pressure evolution of gaseous components of the residual atmosphere during X irradiation was studied with a quadrupole mass spectrometer (Hiden Analytical). Ion peaks of m/e = 1, 2, 14, 16, 18, 28, 32, 44 were monitored with a time increment of 5 s.

After background subtraction, the Al 2p and the O1s−V2p core-level spectra were curve-fitted by mixed Gaussian−Lorentzian lines with due account of the X-ray satellite. The obtained areas under the peaks were used to evaluate the surface composition. The relative atomic sensitivity factors were determined from the reference compounds V_2O_5 and Al_2O_3 to be O(1s):V($2p_{3/2}$):Al(2p) = 1:1.91:0.25. XPS measurements as a function of X irradiation dose were performed for each sample in three series and the patterns were found to be reproducible.

3. Results

3.1. Al_2O_3. A polished sapphire wafer of 0.3-mm thickness was subjected to ultrasonic cleaning in 2-propanol and placed into the spectrometer. Except for a prolonged degassing in a vacuum, no further treatment of the surface was performed. While the fwhm (full width at half-maximum) of the Al 2p core-level peak increases with time of exposure to X-rays, the fwhm of the oxygen peak decreases (Figure 1a). Moreover, the uncorrected binding energy (B.E.) of the O 1s peak drops abruptly in the beginning of X irradiation before increasing slightly later on (Figure 1b, curve 1). On the other hand, the Al 2p peak shifts monotonically to higher B.E.'s (Figure 1b, curve 2). A more quantitative inspection of the original spectra, not shown explicitly, reveals that the O/Al intensity ratio and, therefore, the surface oxygen concentration fall after 35 min of X irradiation before gradually reaching a reduced level at large scatter (Figure 2, curve 1).

To demonstrate the occurrence of surface charging due to exposure to X-rays, the C 1s B.E. of adventitious carbon has been followed constantly with time. Accordingly, an initial jump by more than 0.1 eV (B.E. = 288.4 eV at $t = 0$) is followed by a slower increase. To allow for comparison with the B.E.'s of Al 2p and O 1s, the behavior of C 1s is also presented in Figure

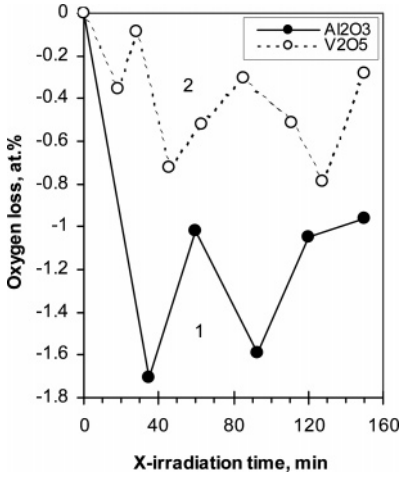

Figure 2. Variation of the surface oxygen concentration in Al_2O_3 (1) and V_2O_5 (2) under X irradiation with reference to nonirradiated samples.

1 (curve 3). The fwhm of the C 1s also increases slightly (not shown) and the carbon content decreases with time of exposure to X-rays, probably because of X-ray induced decomposition and desorption of contaminating hydrocarbons. The modified Auger parameters for oxygen $\alpha'(O) = KE(O\ KLL) + BE(O1s)$ and aluminum $\alpha'(Al) = KE(Al\ KLL) + BE(Al2p)$ vary in the range of 1039.2−1039.0 eV and 1461.4−1461.6 eV, respectively (KE stands for kinetic energy of emitted Auger electrons). No pronounced changes in the valence band of Al_2O_3 have been observed following X irradiation.

Atmospheric humidity causes hydroxyl groups to form on the alumina surface. A significant fraction of surface OH may even survive vacuum-drying above 650 °C as shown in ref 17. With regard to our sample, the asymmetry of the sapphire O 1s peak indicates the occurrence of several oxygen environments. We can assume two O 1s components bound to Al, that is, "bulk lattice" O1 in Al−O−Al and surface O2 in Al−O−H, besides a component O3 (H−O−H) related to water. On the other hand, the symmetrical shape of all Al 2p peaks points to a similarity in the local Al environment (O−Al−O and O−Al−OH). The charge-corrected B.E.'s of O 1s and Al 2p in sapphire are initially 531.5 and 74.8 eV, respectively. This is in the range of typical values measured for Al_2O_3 and $Al(OH)_3$.[18] However, using the C 1s peak for charge correction in studies with alumina surfaces may not be appropriate; instead, a charging-independent parameter, the energy separation between the O 1s and Al 2p peaks E(O−Al), should be considered.[19]

The O 1s spectra obtained at different times of exposure to X-rays were deconvoluted after linear background subtraction by a least squares' fit procedure using symmetrical Gaussian−Lorentzian lines (50/50). Fwhm of all the components contributing to the overall O 1s band were kept constantly equal during deconvolution of the time-dependent spectra. Figure 3a shows the curve-fitted O 1s envelope for the initial surface of sapphire. One can see two major components O1 and O2 with uncorrected B.E.'s of 534.68 and 535.86 eV, respectively, which are in good agreement with those (534.46 eV for Al−O−Al and 535.84 eV for Al−O−H component) of the deconvoluted O 1s spectra obtained for the surface layer of boehmite/pseudoboehmite, AlO(OH), formed on aluminum after hydrothermal treatment.[19] There is also a small O3 peak component (1.3% of the total O 1s area) at 537.84 eV related to adsorbed water molecules. The comparison of Figure 3a and b demonstrates that X irradiation of sapphire gives rise to a change of relative intensities: while the O1 component increases, the O2 component decreases. After irradiation for about 50 min, no contribution due to water is seen to persist. Instead, a new component O4 at 536.9 eV arises and shows no significant changes of the intensity with time (Figure 3b).

The energy separation E(O1s−Al2p) = 456.7 eV for sapphire at zero-time exposure to X-rays is close to E = 456.8 eV as measured for $Al(OH)_3$ after calcination in air at 500 °C.[18] E(O−Al) for the O1, O2, and O4 components in the O 1s spectra for different X-ray exposures are, respectively, 456.43 ± 0.03, 457.63 ± 0.09, and 458.63 ± 0.08 eV. These data may be compared to E(O1−Al) = 456.6 eV and E(O2−Al) = 457.7 eV in $Al(OH)_3$ and to E(O2−Al) = 458.0 eV in AlO(OH) as reported in ref 19. Thus, we attribute the major component O1 to bulk-lattice Al−O−Al bonds in oxide and the component O2 to Al−O−H bonds in a mixture of surface hydroxide and oxyhydroxide or in a partially dehydrated trihydroxide. The origin of the O4 component is not entirely clear. We tentatively ascribe it to isolated hydroxyl groups associated with O═Al−OH type bonds. Figure 3c shows the deconvoluted O 1s spectrum for sapphire subjected to Ar-ion bombardment (500 eV, 30 min) prior to XPS analysis. While surface hydroxide/oxyhydroxide associated with the O2 component is hardly visible (∼1% of the total O 1s signal) after this clean-off procedure, type O4 hydroxyl groups persist (∼4% of the total O 1s signal). This is in agreement with the observation[19] that heating of $Al(OH)_3$ and AlO(OH) films to 300 °C in a vacuum causes decomposition to form γ-Al_2O_3, although complete dehydration is not achieved and residual hydroxyl remains, which supports the above assignment of the O4 component.

The sample composition calculated from the curve-fitting results of the initial O 1s spectrum (Figure 3a) is 67.9%O1−30.8%O2−1.3%O3. Assuming O2 to represent $Al(OH)_3$, the atomic ratio O/Al would be 1.78, while for AlO(OH) it would be 1.59. Using the relative sensitivity factors derived from the O 1s and Al 2p spectra of sputter-cleaned Al_2O_3, the atomic ratio O/Al for the initial surface of sapphire is 1.65. This also allows the surface film to be qualified as a partially dehydrated hydroxide. The thickness of the film is calculated to be about 1.9 nm assuming that it consists of only $Al(OH)_3$.

The change in the surface composition of Al_2O_3 because of X irradiation represented by fractions of oxide (O1), hydroxide/oxyhydroxide (O2), and isolated hydroxyls (O4) is shown in Figure 4 along with the variation of E(O1s−Al2p). The effect of X-rays on the spectra parameters can now be interpreted as follows. Already, low X-ray doses cause dehydration of the surface. This is reflected in a loss of surface oxygen (Figure 2) and in a drop of the B.E. of the overall O 1s peak (Figure 1b). In agreement with observations made in ref 19, dehydration results in surface charging (Figure 1b). The removal of terminal OH/water (and adventitious carbon) seems to be responsible for the relatively strong changes of the B.E. in the initial stages of X irradiation. The B.E.'s of the Al 2p (Figure 1b, curve 2) and the O1 component (Figure 1b, curve 4), both reflecting bonds that are not surface-terminating, follow a similar trend which becomes clearly visible after about 60 min time of exposure to X-rays. Because of the decomposition of the surface hydroxide, the fwhm of the O 1s peak (Figure 1a) and the separation E(O−Al) (Figure 4, curve 4) monotonically decrease.

Ion bombardment efficiently cleans the surface of Al_2O_3, thereby completely removing carbon contamination and $Al(OH)_3$/AlO(OH) (Figure 3c). For such a surface, the initial charging during XPS is higher than after X irradiation, and E(O−Al) = 456.2 eV, $\alpha'(O)$ = 1039.0 eV, and $\alpha'(Al)$ = 1461.7 eV. X

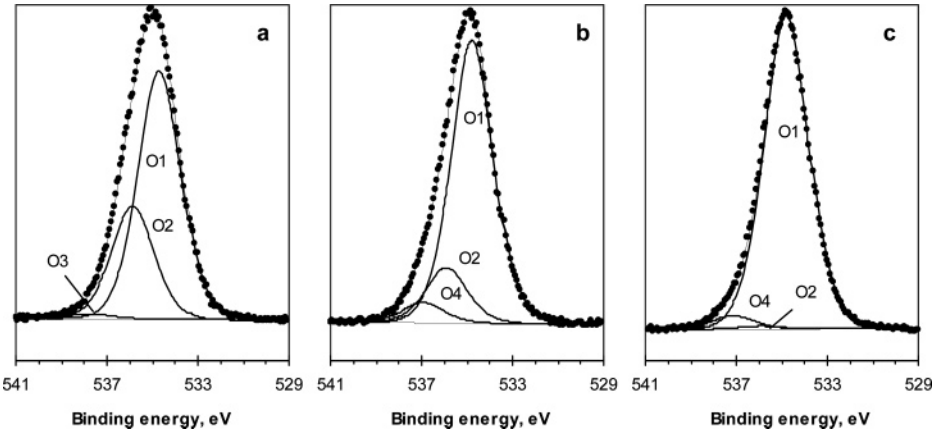

Figure 3. Deconvoluted O 1s spectra of Al_2O_3 in the initial state (a) (zero X-ray exposure or nonirradiated sample), after X irradiation for 150 min (b), and after 500 eV Ar^+-ion bombardment for 30 min (c). The components O1, O2, O3, and O4 in the O 1s envelope represent Al−O−Al, Al−O−H, and H−O−H environments and residual hydroxyls, respectively. No charging correction for B.E. is applied.

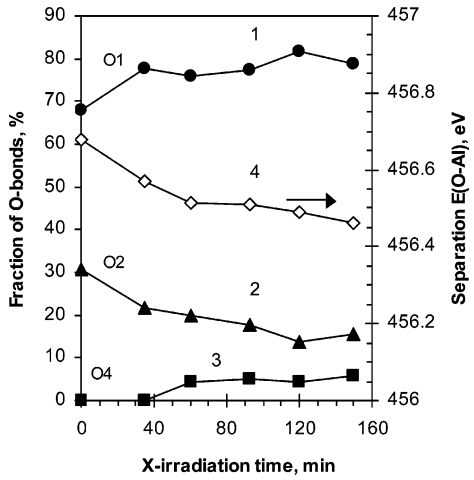

Figure 4. Variation of the surface phase composition represented by the fractions of oxide O1 (1), hydroxide O2 (2), and isolated hydroxyl groups O4 (3) during X-ray irradiation of Al_2O_3. The change in the energy separation between the O 1s and Al 2p peaks, E(O−Al), is also shown (4).

irradiation of sputter-cleaned Al_2O_3 during 1 h causes no noticeable changes of the XPS peaks.

3.2. V_2O_5. Figure 5a (curve 1) shows the zero-time XPS spectrum of the O1s−V2p region (scan time 73 s) for a compacted sample of vanadium pentoxide. Binding energies and widths of the V $2p_{3/2}$ (E_b = 517.0 eV, fwhm = 1.4 eV) and O 1s peaks (E_b = 529.8 eV, fwhm = 1.6 eV) are in good agreement with those of Mendialdua et al.[12] V_2O_5 loses some oxygen because of irradiation; the effect is yet less strong than for sapphire (Figure 2). In contrast to Al_2O_3, continual X irradiation changes neither fwhm nor B.E. of the O 1s peak in V_2O_5 (Figure 6a, b, curve 1). The oxygen Auger parameter α'(O) turns out to be more sensitive to irradiation and decreases nearly linearly in the range of 1043.2−1042.7 eV. On the other hand, the V $2p_{3/2}$ peak broadens (by ∼0.2 eV after 2.5 h of X irradiation, see Figure 6a) to develop a small contribution at low B.E. after maximum time of exposure (Figure 5a, curve 2). At the same time, the B.E. of the V $2p_{3/2}$ peak slightly decreases and the energy separation E(O−V$2p_{3/2}$) increases, respectively (Figure 6b, curves 2, 3). The vanadium Auger parameters, α_1'(V) = KE(V *LMV*) + BE(V$2p_{3/2}$) and α_2'(V) = KE(V *LMM*) + BE(V$2p_{3/2}$), are at ∼984.4 and 944.3 eV, respectively. No charging is noticed during XPS analysis of V_2O_5, however, similar to reports in ref 12, the C 1s peak, in contrast to other peaks, exhibits a continuous shift to higher B.E.'s by up to ∼0.25 eV (Figure 6b, curve 4).

The loss of lattice oxygen under X irradiation results in a change of the vanadium oxidation state as indicated by the broadening of the V $2p_{3/2}$ peak and by the appearance of the low B.E. contribution. Deconvolution of the V $2p_{3/2}$ peak in irradiated V_2O_5 reveals a new component (Figure 5b, curve 2) whose B.E. is 1.25 eV lower than that of the major peak (the latter obviously corresponding to the V^{5+} state). The fraction of this component increases with irradiation dose and reaches about 8% (of the total V $2p_{3/2}$ signal) at maximum time of exposure to X-rays. According to the literature,[20,21] the difference in B.E.'s because of variations in the vanadium oxidation state shows large scatter and is between 0.7 and 2.0 eV for ΔB.E.($V^{5+}-V^{4+}$) and between 1.2 and 2.0 eV for ΔB.E.($V^{5+}-V^{3+}$) which may introduce uncertainties in peak assignments. The position of the low-energy component at 515.75 eV as derived from curve fitting and its 1.25 eV shift with respect to the major peak at 517.00 eV are close to the V^{4+} binding energy of 515.65 eV and ΔB.E.($V^{5+}-V^{4+}$) = 1.35 eV determined in ref 12 for VO_2. Other papers have reported similar values of ΔB.E.($V^{5+}-V^{4+}$) after deconvolution of the V $2p_{3/2}$ peak. Accordingly, the V^{4+} component arising because of reductive treatment of the V_2O_5/Al_2O_3 catalyst with H_2, CH_4, and CO was shifted by 1 eV with respect to V^{5+}.[22] Finally, in studies of thermal reduction of V_2O_5(001)[23] and calcination of $V_2O_5/La_2O_3-TiO_2$,[24] ΔB.E.($V^{5+}-V^{4+}$) values of 1.35 and 1.4 eV, respectively, were obtained. Thus, we conclude that the X irradiation-induced oxidation state at low B.E. (Figure 5b) can be reasonably assigned to V^{4+}. We believe that the reduction involves desorption of relatively loosely bound oxygen, that is, surface vanadyl oxygen as also proposed in ref 10.

Oxidation states lower than V^{4+} may be produced in V_2O_5 by ion irradiation, which causes preferential sputtering of oxygen. As can be seen from Figure 5a, 500 eV Ar^+ bombardment of V_2O_5 for 30 min (ion dose of about $1.5\cdot10^{16}$ ions/cm^2) causes a substantial modification of the V2p−O1s spectrum (curve 3). Deconvolution of the broad V $2p_{3/2}$ line shows that, in addition to V^{4+}, another intense component emerges at a B.E. of 515.2 eV (Figure 5b, curve 3) with an energy difference of 1.91 eV with respect to V^{5+}. This value is close to the values reported in refs 12 and 25 for V_2O_3, and thus the peak may be ascribed to V^{3+}. Ar^+ bombardment seems to produce even small amounts of V^{2+} as concluded from the occurrence of a component at B.E. = 513.7 eV which is close to that reported for VO.[25] The fractions of V^{4+}, V^{3+}, and V^{2+} in Figure 5b are,

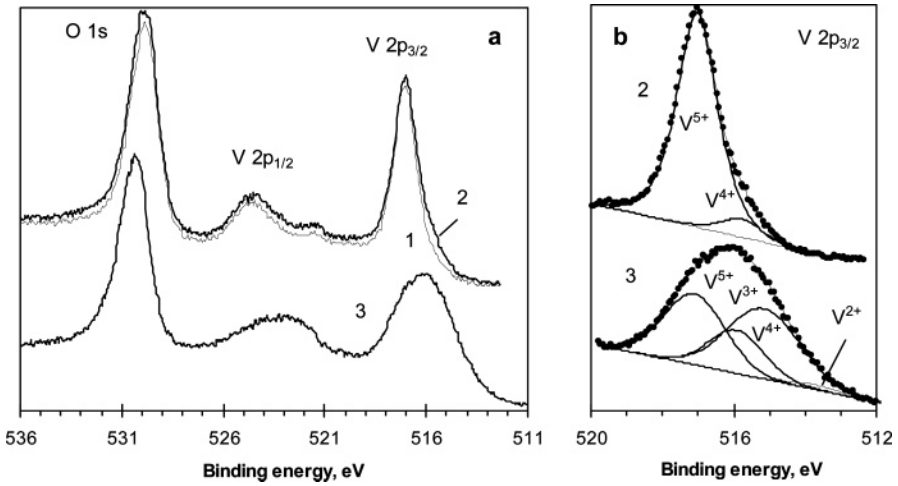

Figure 5. (a) XP spectra (O 1s−V 2p region) of V_2O_5 in the initial state (1) (zero exposure or nonirradiated sample), after X-ray irradiation for 150 min (2), and after 500 eV Ar^+ bombardment for 30 min (3). (b) Deconvolution of the V $2p_{3/2}$ peak for V_2O_5 irradiated with X-rays for 150 min (2) and with 500 eV Ar^+ ions for 30 min (3).

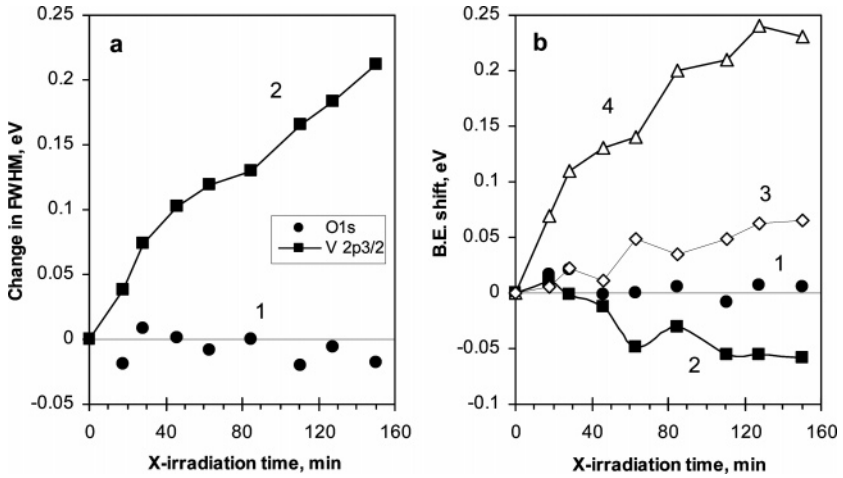

Figure 6. Change in fwhm (a) and binding energy shift (b) for the O 1s (1), V $2p_{3/2}$ (2), and C 1s (4) peaks as a function of time of X-ray irradiation of V_2O_5 with reference to nonirradiated sample. The change in the energy separation between the O1s and V$2p_{3/2}$ peaks, E(O−V), is also shown (3).

respectively, 20.5, 41.3, and 1.6%. This leads to an average vanadium oxidation state of ∼3.9 for vanadium in ion-irradiated V_2O_5. After Ar^+ bombardment, the separation E(O1s−V$2p_{3/2}$), which is sensitive to the vanadium oxidation state,[12] significantly increases as compared to that after X irradiation (14.2 and 12.9 eV, respectively).

In view of the small fraction of reduced species produced by X irradiation, we have not observed any appreciable distinctions in the valence band spectrum of irradiated V_2O_5. By using He−UPS, some changes in the region of the O 2p bonding orbitals were found[10] for V_2O_5(001) after 30 min of Mg K_α X irradiation. However, after ion bombardment of our sample, the valence band spectrum changes dramatically. The O 2p band shifts away from the Fermi level by about 0.6 eV, and a pronounced peak related to the emission from defect-induced V 3d states arises near E_F indicating the presence of reduced V states. The spectrum, not shown here, agrees well with the XPS valence band spectrum reported in ref 26 for VO_2.

The X-ray induced damage in V_2O_5 is partly removed with time while keeping the sample under vacuum. For example, the zero-time XP spectrum taken after holding V_2O_5 for 24 h at a base pressure of $8{\cdot}10^{-10}$ mbar, following X-ray exposure during 170 min, was seen to correspond to one obtained after exposure of the fresh sample to X-rays for 80 min. Obviously, some reconstruction associated with low activation energy was in operation to produce this result. However, further irradiation of reconstructed V_2O_5 caused much faster and stronger spectral changes than observed in the first series of time-dependent X-ray measurements. Despite the low amount of reduced species in irradiated V_2O_5, some darkening of the sample could be observed which, however, vanished after several days of exposure to air.

3.3. V−Al−O Catalyst. The O1s−V2p spectrum of the compacted powder of V−Al−O is shown in Figure 7 using a charge-corrected binding energy scale. It is seen that even for zero-time exposure to X-rays (curve 1), the fwhm of the V $2p_{3/2}$ peak (2.33 eV) is significantly larger than for V_2O_5 (1.41 eV). This indicates the presence of vanadium oxidation states lower than +5. The Al 2p peak is also broader (2.38 eV) than in Al_2O_3 (1.9 eV) and, finally, the O 1s peak in V−Al−O (fwhm 3.6 eV) is much broader than in both V_2O_5 (1.6 eV) and Al_2O_3 (2.68 eV). Obviously, a variety of oxygen environments has to be considered in the deconvolution of the O1s−V2p spectra. In fact, at least three most abundant local oxygen configurations, Al−O−Al, V−O−V, and Al−O−H, are needed for peak fitting; they correspond to the components O1, O2, and O3, respectively. The B.E.'s of the latter two, O2 and O3, are shifted by −1.5 and +1.2 eV with respect to O1; for details, see the data presented in sections 3.1 and 3.2. It is found that the initial state composition of the V−Al−O catalyst contains a mixture

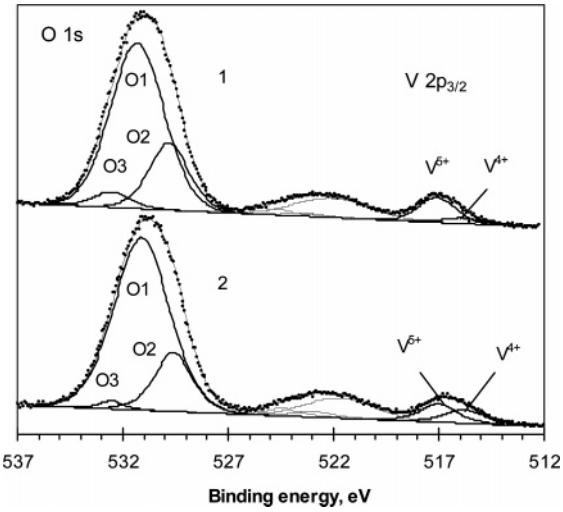

Figure 7. Deconvoluted XP spectra (O 1s−V 2p region) of aluminovanadate oxide V−Al−O in the initial state (1) (zero X-ray exposure or nonirradiated sample) and after X irradiation for 150 min (2). The components O1, O2, and O3 in the O 1s envelope represent Al−O−Al, V−O−V, and Al−O−H environments, respectively. The binding energy scale is charge-corrected.

of 80% V^{5+} and 20% V^{4+} (Figure 7, curve 1), that is, the average V formal oxidation state is +4.8. The ratio of V−O−V to Al−O−Al configurations is O2/O1 ∼ 0.3 which is close to the bulk value (atomic ratio V/Al = 0.25). The oxygen Auger parameter $\alpha'(O) = 1039.3$ eV turns out to be noticeably different from that of V_2O_5 (1043.2 eV) but close to $\alpha'(O)$ of Al_2O_3 (1039.0 eV) indicating dominating Al−O−Al environments.

The effect of X irradiation is much more pronounced for V−Al−O than for Al_2O_3 and V_2O_5. With increasing time of exposure to X-rays, there is a small yet steady increase in both fwhm and B.E. of O 1s and Al 2p peaks (Figure 8, curves 1, 2). The energy separation E(O−V) thereby increases in the range 14.07−14.31 eV. A substantial broadening and shift of the V $2p_{3/2}$ peak to lower B.E.'s (Figure 8, curve 3) is seen which exceeds by far the corresponding changes in the V $2p_{3/2}$ peak of the X irradiated V_2O_5 (Figure 6, curve 2). The fraction of V^{4+} rises and attains about 45% at maximum time of exposure (Figure 7, curve 2). At the same time, the population of V−O−V bonds decreases (the ratio O2/O1 drops to ∼0.23) and the fraction of Al−O−H bonds reduces from 5 to 1.5% (Figure 7).

The behavior of the low B.E. O 2s and V 3p peaks resembles that of O 1s and V 2p. While the O 2s peak experiences minor changes, the V 3p peak clearly displays a noticeable broadening and shift to lower B.E.'s with time of exposure to X-rays (Figure 8, curve 4). The difference in kinetic energy of V $2p_{3/2}$ and V 3p electrons (737 and 1212 eV, respectively) shows that X-ray induced chemical modifications extend at least to a depth sampled by the V 3p electrons. The sampling depth, equal to $\sim 3\lambda$ (λ is the inelastic mean free path),[27] contributes to 95% of the total peak intensity and has been calculated to be 11.8−13.2 nm and 15.2−16.8 nm for V 2p and V 3p electrons, respectively (ranges reflect uncertainty in the density of V−Al−O).

In contrast to the main components, the C 1s peak shifts to noticeably higher B.E.'s during irradiation (Figure 8b, curve 5). The behavior is similar to that observed for V_2O_5 (Figure 6b, curve 4). The sample surface obviously experiences positive charging with time, and the shift of the C 1s peak might be related to adventitious carbon serving as charge-trapping sites.[28]

The initial surface composition of the catalyst has been evaluated to contain 4.7 V, 26.1 Al, and 69.2 O (in at. %). X irradiation causes the oxygen concentration to decrease and the surface to slightly enrich in Al (Figure 9). The strongest change in the surface concentration occurs during the first 60 min of exposure to X-rays. As compared to V_2O_5 (Figure 2), the loss of oxygen in V−Al−O is somewhat larger. X irradiation also causes some desorption of carbon contamination (Figure 9, curve 4).

Gas evolution during X irradiation of V−Al−O monitored by a quadrupole mass spectrometer is shown in Figure 10. It is seen that with the onset of irradiation the level of oxygen and carbon-containing molecules in the residual atmosphere (characterized by ion peaks O^+, CO^+, curves 1, 2) sharply rises before rapidly leveling off. Distinct from this behavior, the H_2O^+ intensity (like OH^+ and H^+) gradually increases and attains a steady-state level after about 60−80 min of X irradiation (Figure 10, curve 3). To assess the effect of heating, the temperature at the sample surface has been monitored during X-ray exposure. As can be seen from Figure 10 (curve 4), after 80−90 min the temperature has reached a stable level of ∼36 °C. Thus, the overall temperature elevation amounted to about 10 °C. Irradiation was terminated after 210 min by moving the sample away from the X-ray source; this caused the intensities of all gas components and also the temperature to drop (Figure 10). As a result of X-ray irradiation, the color of the sample surface turned from green-yellow to brownish.

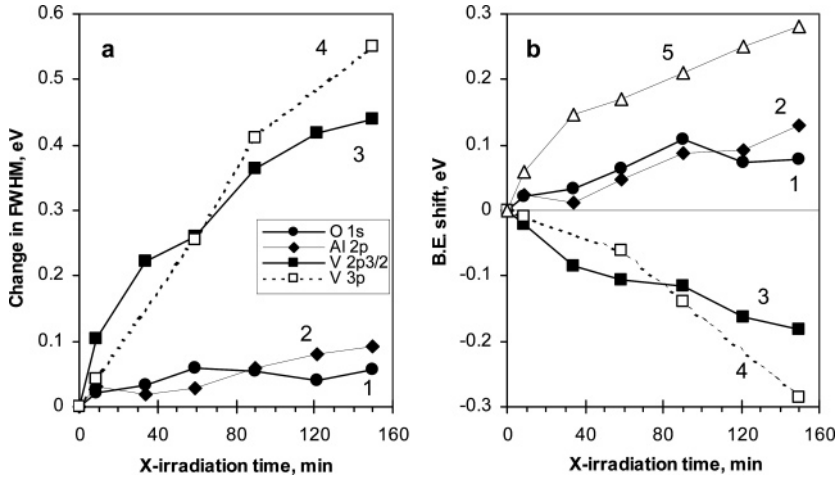

Figure 8. Change in fwhm (a) and binding energy shift (b) for the O 1s (1), Al 2p (2), V $2p_{3/2}$ (3), V 3p (4), and C 1s (5) peaks as a function of time of exposure to X-rays of aluminovanadate oxide, V−Al−O, with reference to nonirradiated sample.

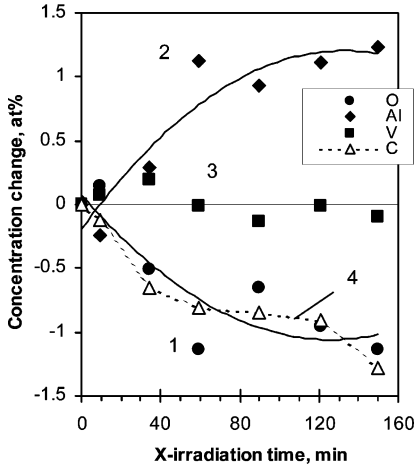

Figure 9. Variation of the surface concentration of oxygen (1), aluminum (2), vanadium (3), and carbon (4) in V−Al−O during X irradiation with reference to nonirradiated sample.

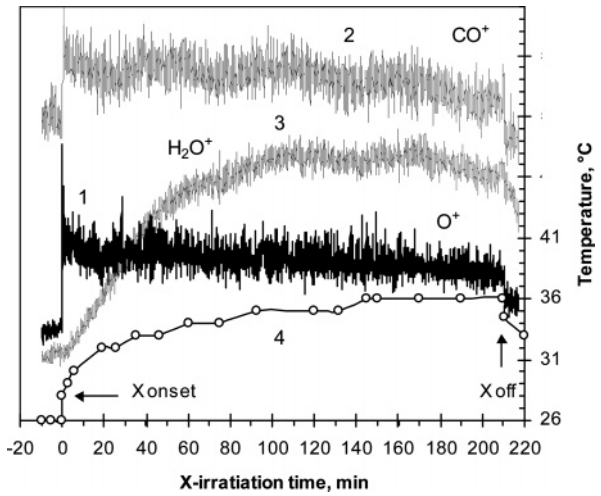

Figure 10. Variation of the level of gas components represented by ion peaks O^+ (1), CO^+ (2), and H_2O^+ (3) in the mass spectrum of the residual gas atmosphere before, during, and after termination of X irradiation of aluminovanadate oxide, V−Al−O. The variation of the temperature (4) at the surface of V−Al−O is also presented.

4. Discussion

We start by inspecting in detail the X-ray induced degradation process of V−Al−O catalysts which can be depictured as follows. According to the literature,[16] the catalyst structure at a given pH = 7.5 may be described as a polymer linking of $[VO_x]^{n-}$ units containing vanadium in tetrahedral environment, supported on amorphous aluminum hydroxide. The onset of irradiation causes immediate desorption of chemisorbed and loosely bound lattice oxygen (Figure 10, curve 1). Irradiation affects preferentially the vanadium oxide subsystem and breaks V−O−V bonds thus decreasing their abundance (Figure 7). Accumulating damage brings about reduction of V^{5+}, the amount of the initially available V^{4+} species grows by a factor of more than 2, and the average vanadium oxidation state in the catalyst reaches a value of +4.55. The dark color of the irradiated surface also indicates abundant formation of V^{4+} species because all vanadium oxides containing vanadium in an oxidation state lower than +5 are black. As a result, the V $2p_{3/2}$ peak appreciably broadens and shifts to lower B.E.'s (Figure 8). The final V $2p_{3/2}$ B.E. corresponds to that reported for V_4O_9.[12]

There seems to be little agreement in the literature regarding the X-ray induced in-depth damage of materials; the discussion on CeO_2 provides an example.[6,7] According to our results, on the basis of the behavior of the V 3p peak in V−Al−O, the damage pervades the layer to a depth that corresponds at least to the escape length of the V 3p electrons. This length is estimated as being about 16 nm.

X irradiation of V−Al−O also causes breaking of Al−O−H bonds (Figure 7) and decomposition of aluminum hydroxide. This is corroborated by changes in fwhm and B.E. of the Al 2p peak which resemble those of X irradiated Al_2O_3 covered by a hydroxide film (cf. Figures 8 and 1). At the same time, the changes in the Al 2p spectra indicate that dehydration is, as expected, not accompanied by reduction of aluminum ions. The desorption of hydroxyl/water molecules from the surface is retarded because of diffusion-limited mass transport in catalyst pores; the intensities of characteristic ions (OH^+, H_2O^+) in the mass spectrum of the residual gas atmosphere thus increase only slowly (Figure 10, curve 3). The surface oxygen concentration decreases respectively (Figure 9, curve 1) implying that hydroxyl association to form water can significantly contribute to the total oxygen loss.

X-ray induced damage in Al_2O_3, V_2O_5, and V−Al−O has been seen to increase in order of mention. Alumina with a native hydroxide film obviously suffers dehydration under X-ray exposure; clean Al_2O_3, however, remains rather unaffected by prolonged X irradiation. Vanadium pentoxide turns out to be more sensitive to X-rays than Al_2O_3 and experiences some reduction to the V^{4+} state. The major difference between Al_2O_3 and V_2O_5 in resisting X irradiation may originate from the crystal structure, which is ionic with long-range order in alumina and (predominantly) molecular with more local order in V_2O_5. The V−Al−O catalyst proves to be most susceptible to X-rays and is easily damaged even by low doses. The damage involves the vanadium oxide and aluminum hydroxide subsystems and results in a substantial reduction of V^{5+} to V^{4+}, dehydration, and loss of oxygen. The changes in the vanadium oxide subsystem of V−Al−O are faster than in V_2O_5 as indicated by the variation with time of the V $2p_{3/2}$ peak features. Indeed, the same changes of both fwhm and B.E. of the V $2p_{3/2}$ peak, which occurred for V_2O_5 after 150 min of X irradiation, were observed in V−Al−O already after about 30 min of exposure (cf. Figures 6, 8). The different reducibility of vanadium in the two oxides can be explained by differences in their structure. Accordingly, vanadium in octahedral environment is more stable with respect to reduction than vanadium in tetrahedral environment as present in V−Al−O.

Another important issue concerns the effect of Al atoms on the reducibility of vanadium. It has been observed[14] that the B.E. of V $2p_{3/2}$ in ternary $V_2O_5-WO_3/TiO_2$ catalysts is lower than in binary V_2O_5/TiO_2 catalysts. Obviously, the reducibility of V^{5+} to V^{4+} is enhanced by tungsten. In fact, temperature-programmed reduction (TPR) of $V_2O_5-WO_3/TiO_2$ differs from that of both V_2O_5/TiO_2 and WO_3/TiO_2 and implies the occurrence of an interaction between vanadia and tungsta species. In our case, the presence of Al atoms and the existence of V−O−Al^{3+} configurations should affect the electronic density distribution around vanadium and oxygen atoms. The ionic character of the (predominantly covalent) V−O bond and, consequently, the acid−base properties and the reducibility of the system are thus expected to change.[29] The lower electronegativity of aluminum as compared to vanadium would render the latter less electrophilic in the V−O−Al^{3+} unit than in the V−O−V bond configurations. The reduction temperature obtained in TPR of the V−Al−O catalyst was lower than that for V_2O_5, which also points to a higher reducibility of V^{5+} in V−Al−O and is

consistent with the higher sensitivity to X-rays as compared to V_2O_5.

Intense local heating of the surface by X irradiation has been considered the main damaging factor to explain the reduction of ceria.[4,5] In our experiments, we can exclude thermally induced processes to be dominating. Neither the desorption of surface hydroxyl nor the reduction of vanadium can be explained in this manner since the temperature at the surface of V−Al−O after irradiation for 3 h does not exceed 36 °C. Apparently, other mechanisms involving electronic rearrangements must be invoked.[5,6]

Two main mechanisms of radiation damage may be considered to account for the observed effects of X-ray irradiation in oxides: electron−hole pair generation and Auger decay.[28] Photo- and secondary electrons propagating in a solid experience energy losses and, given enough energy, can excite valence band electrons toward the conduction band. Such inelastic processes lead to the generation of electron−hole pairs within the penetration depth of X-rays. From the physical point of view, a hole in the valence band of an insulator corresponds to a bond being broken between two atoms (metal and oxygen in oxides). Electrons resulting from electron−hole pair generation and escaping from the surface into the vacuum leave a positively charged surface layer. Consequently, the arising electric field reduces the probability of electron−hole recombination. This factor may also contribute to explain the stronger damage in insulating V−Al−O as compared to V_2O_5.

Photoionization of electron core levels followed by an Auger decay provides an alternative process encountered in XPS. The Auger mechanism leaves at least two holes in the valence band and, in contrast to metals, the electroneutrality cannot be quickly restored on and around the excited atoms because of the lack of conduction electrons in insulators. In oxides, the Auger decay which follows photoionization of the O 1s level produces two holes in the valence band, while the Auger cascade following ionization of the metal 1s level (for Al) or 2s level (for V) may leave multiple holes in the same valence band. The X-ray induced V $L_3M_{23}M_{45}$ Auger spectra of the V−Al−O catalyst show the valence band O 2p and V 3d electrons to be involved in the decay. Multiple hole states in the valence band break bonds between V and O (or between Al and OH) which leads to reduction of vanadium and to subsequent desorption of oxygen as a neutral molecule. Both electron−hole pair generation and Auger decay may occur up to the penetration depth of X-rays.[28] This is why irradiation-induced reduction of vanadium could be observed within the sampling depth of the V 3p electrons.

5. Conclusions

The interaction of Mg K_α radiation with Al_2O_3, V_2O_5, and V−Al−O causes modifications of the surface composition and, eventually, of the metal oxidation state. The extent to which such modifications occur depends on the nature and structure of the oxide. The native hydroxide film formed because of contact of air humidity with Al_2O_3 is efficiently removed by exposure to X-rays. Nearly complete dehydration is achieved by Ar^+-bombardment. Clean Al_2O_3 demonstrates a rather high resistance to prolonged X irradiation. V_2O_5 loses some oxygen and V^{5+} reduces to the V^{4+} state on interaction with Mg K_α radiation. The fraction of V^{4+} species amounts to ∼8% after 150 min of exposure. Lower vanadium oxidation states, V^{3+} and V^{2+}, arise in V_2O_5 after Ar^+ bombardment. X-ray induced damage in V_2O_5 can be removed by exposing the oxide to air.

Aluminovanadate oxide, V−Al−O, demonstrates the largest sensitivity to X-rays, displaying degradation already at low doses. Irradiation of the catalyst results in a decrease of the oxygen surface concentration and in an appreciable reduction of the vanadium mean oxidation state. The fraction of the V^{4+} species initially present in the oxide increases from ∼20 to ∼45%. Aluminum hydroxide in V−Al−O also decomposes, as also in the case of Al_2O_3. As a result of the overall modifications, the color of the sample surface changes. With the onset of X irradiation, an immediate rise of the level of oxygen molecules in the residual atmosphere is observed along with a gradual increase of the amount of desorbed water molecules. The effect of heating can be excluded to account for the observed changes since the temperature on the surface during irradiation does not exceed 36 °C. The damage is believed to be caused by the electron−hole pair generation and Auger decay and extends to a significant depth. In view of the high susceptibility of V−Al−O to X-rays, short-time XPS analysis of such catalysts is mandatory to obtain information on the original chemical composition.

Acknowledgment. The authors thank the Direction Générale des Technologies, de la Recherche et de l'Énergie de la Région Wallonne (GREDECAT) for the financial support and N. Blangenois for her help in the preparation of the V−Al−O catalyst.

References and Notes

(1) Goodman, D. W. *J. Vac. Sci. Technol., A* **1996**, *14*, 1526.
(2) Singh, N. K.; Baker, B. G. *Characterization of catalysts by surface analysis*; Springer Series in Surface Sciences: Berlin-Heidelberg-New York, 2003; Vol. 23, p 405.
(3) Grimblot, J.; Bonnelle, J. P. *C. R. Séances Acad. Sci., Ser. C* **1976**, *282*, 399.
(4) Paparazzo, E. *Surf. Sci.* **1990**, *234*, L253.
(5) Paparazzo, E.; Ingo, G. M.; Zacchetti, N. *J. Vac. Sci. Technol., A* **1991**, *9*, 1416.
(6) Rama Rao, M. V.; Shripathi, T. *J. Electron Spectrosc. Relat. Phenom.* **1997**, *87*, 121.
(7) Paparazzo, E.; Ingo, G. M. *J. Electron Spectrosc. Relat. Phenom.* **1998**, *95*, 301.
(8) Suoninen, E.; Minni, E.; Curelaru, I. M. *J. Microsc. Spectrosc. Electron.* **1981**, *6*, 1.
(9) Tompkins, H. G.; Curelaru, I. M.; Din, K. S.; Suoninen, E. *Appl. Surf. Sci.* **1985**, *21*, 280.
(10) Zhang, Z.; Henrich, V. E. *Surf. Sci.* **1994**, *321*, 133.
(11) Suzer, S. *Appl. Spectrosc.* **2000**, *54*, 1716.
(12) Mendialdua, J.; Casanova, R.; Barbaux, Y. *J. Electron Spectrosc. Relat. Phenom.* **1995**, *71*, 249.
(13) Bukhtiyarov, V. I. *Catal. Today* **2000**, *56*, 403.
(14) Reiche, M. A.; Bürgi, T.; Baiker, A.; Scholz, A.; Schnyder, B.; Wokaun, A. *Appl. Catal., A* **2000**, *198*, 155.
(15) Wiame, H.; Bois, L.; Lharidon, P.; Laurent, Y.; Grange, P. *Solid State Ionics* **1997**, *101−103*, 755.
(16) Blangenois, N.; Florea, M.; Grange, P.; Prada Silvy, R.; Chenakin, S. P.; Bastin, J.-M.; Kruse, N.; Barbero, B. P.; Cadús, L. *Appl. Catal., A* **2004**, *263*, 163.
(17) Peri, J. B. *J. Phys. Chem.* **1965**, *69*, 211.
(18) Rueda, F.; Mendialdua, J.; Rodriguez, A.; Casanova, R.; Barbaux, Y.; Gengembre, L.; Jalowiecki, L. *J. Electron Spectrosc. Relat. Phenom.* **1996**, *82*, 135.
(19) Alexander, M. R.; Thompson, G. E.; Beamson, G. *Surf. Interface Anal.* **2000**, *29*, 468.
(20) Eberhardt, M. A.; Proctor, A.; Houalla, M.; Hercules, D. M. *J. Catal.* **1996**, *160*, 27.
(21) Chen, Y.; Xie, K.; Liu, Z. X. *Appl. Surf. Sci.* **1998**, *133*, 221.
(22) Harlin, M. E.; Niemi, V. M.; Krause, A. O. I. *J. Catal.* **2000**, *195*, 67.
(23) Devriendt, K.; Poelman, H.; Fiermans, L. *Surf. Sci.* **1999**, *433−435*, 734.
(24) Reddy, B. M.; Sreekanth, P. M.; Reddy, E. P.; Yamada, Y.; Xu, Q.; Sakurai, H.; Kobayashi, T. J. *Phys. Chem. B* **2002**, *106*, 5695.
(25) Della Negra, M.; Sambi, M.; Granozzi, G. *Surf. Sci.* **1999**, *436*, 227.
(26) Demeter, M.; Neumann, M.; Reichelt, W. *Surf. Sci.* **2000**, *454−456*, 41.
(27) *Handbook of X-ray and ultraviolet photoelectron spectroscopy*; Briggs, D., Ed.; Heyden: London, 1977; p 158.
(28) Cazaux, J. *J. Electron Spectrosc. Relat. Phenom.* **1999**, *105*, 155.
(29) Grzybowska-Świerkosz, B. *Appl. Catal., A* **1997**, *157*, 409.